EAST EUROPEAN JOURNAL OF PHYSICS. 2. 445-460 (2026)
DOI:10.26565/2312-4334-2026-2-50 ISSN 2312-4334

AMBIPOLAR DIFFUSION AND ELECTRIC FIELD REVERSAL IN ELECTRONEGATIVE PLASMA WITH CHARGED NANOPARTICLES

V. Lisovskiy*, S. Dudin, S. Bogatyrenko, S. Rezunenko, V. Yegorenkov
V.N. Karazin Kharkiv National University, 4 Svobody Sq., Kharkiv, 61022, Ukraine
**Corresponding Author email: lisovskiy@karazin.ua*
Received February 25, 2026; revised April 18, 2026; accepted May 20, 2026

An analytical model of ambipolar diffusion in plasma consisting of electrons, positive ions, negative ions, and negatively charged nanoparticles is proposed. Analytical expressions are derived for the ambipolar diffusion coefficients of all charged species, as well as for the ambipolar electric field strength. In plasma containing only electrons, positive ions, and negative ions, high concentrations of negative ions lead to a transition from ambipolar to free diffusion, where the ambipolar diffusion coefficients approach the corresponding free diffusion coefficients. In plasma consisting of electrons, positive ions, and negatively charged nanoparticles, high nanoparticle concentrations result in qualitatively different behavior: the ambipolar diffusion coefficient of electrons approaches twice the free electron diffusion coefficient, while the ambipolar diffusion coefficient of positive ions approaches twice the free diffusion coefficient of nanoparticles. For the general four-component plasma, the ambipolar diffusion regime is governed by the dominant electron-loss mechanism, namely, electron attachment to either electronegative gas molecules or nanoparticles. If electron attachment to gas molecules dominates, the ambipolar diffusion coefficients of electrons, negative ions, and nanoparticles remain close to their free diffusion coefficients. In contrast, when electron attachment to nanoparticles dominates, these coefficients approach twice the corresponding free diffusion coefficients. The ambipolar diffusion coefficient of positive ions was found to depend strongly on the dominant negatively charged species in plasma. Under intensive negative-ion formation, it approaches the free diffusion coefficient of negative ions, whereas in plasma dominated by electron attachment to nanoparticles it asymptotically approaches twice the free diffusion coefficient of nanoparticles. It is shown that sufficiently high concentrations of negative ions and/or charged nanoparticles substantially reduce the ambipolar electric field strength and may even reverse its sign. A weakly negative ambipolar electric field can remove excess negative ions and nanoparticles from plasma, thereby stabilizing the discharge. Experiments with acetylene plasma demonstrated intense transport of small nanoparticles toward the tube walls, which may serve as indirect evidence of an ambipolar electric-field reversal.
Keywords: *Ambipolar diffusion; Analytic model; Ambipolar electric field; Nanoparticles; Negative ions*
PACS: 52.80.Pi, 52.50.Qt, 52.65.Kj

INTRODUCTION

Gas-discharge plasma has found extremely broad application in modern technology and everyday life. At present, its use is no longer limited to hardening of metal surfaces and fabrication of microelectronic devices, as was the case several decades ago. A vast number of products and materials currently in use are either manufactured or modified using gas-discharge plasma. In addition, new research directions have emerged, including “plasma medicine” [1,2] and “plasma agriculture” [2–6]. Consequently, investigations of the processes governing the maintenance and transport properties of gas-discharge plasmas under various conditions remain highly relevant.

Quasineutral plasma is typically composed of electrons and positive ions with approximately equal concentrations, $n_e = n_+$, moving in a neutral gas background. Diffusion tends to smooth concentration gradients of charged particles. When the charged-particle density is sufficiently low, for example $n_e < 10^6$ cm^{-3}, electrons and positive ions diffuse almost independently and do not significantly affect each other’s motion. Such diffusion is referred to as free diffusion, and the corresponding diffusion coefficients of electrons and positive ions are denoted by D_e and D_+, respectively.

The situation changes when the charged-particle density increases to $n_e > 10^8$ cm^{-3}, at which point free diffusion transitions to ambipolar diffusion. Because electrons possess a mobility μ_e much higher than the mobility of positive ions μ_+, their diffusion coefficient is also significantly larger, i.e., $D_e >> D_+$. As a result, the more mobile electrons, particularly those with higher energies, tend to escape from the plasma volume. In a gas-discharge chamber, these electrons are absorbed by the tube walls, charging them negatively. Consequently, the plasma acquires a positive space charge, and charge separation gives rise to the so-called ambipolar electric field. This field attracts positive ions toward the negatively charged wall and repels low-energy electrons away from it. Therefore, the fluxes of positive ions and electrons arriving at the wall become nearly equal. A positive ion reaching the wall recombines with one of the electrons accumulated there, while another energetic electron subsequently arrives, restoring the negative wall charge.

The first expressions for the ambipolar diffusion coefficient D_a and the corresponding ambipolar electric field were derived by Walter Schottky [7,8], who developed the theory of the positive column in electropositive quasineutral plasma, where $n_e = n_+$. In this case, both electrons and positive ions diffuse with the same ambipolar diffusion coefficient D_a.

Cite as: V. Lisovskiy, S. Dudin, S. Bogatyrenko, S. Rezunenko, V. Yegorenkov, East Eur. J. Phys. 2, 445 (2026), https://doi.org/10.26565/2312-4334-2026-2-50

However, many plasma technologies employ so-called electronegative gases, whose molecules capture free electrons and form molecular negative ions (e.g., SF_6^-, O_2^-, or produce atomic negative ions (F^-, H^-, O^-) through dissociative attachment processes [9–13]. Such negative ions may be directly accelerated, for example, for plasma heating purposes [14–19], and they also participate in various plasma-chemical processes [20–24]. Therefore, electronegative plasmas have attracted considerable attention from researchers [25–37].

The formation of negative ions represents a loss mechanism for free electrons, since negative ions in gas-discharge plasma generally cannot acquire sufficient energy to ionize gas molecules and, due to their low mobility, carry only a negligible electric current. In addition, negative ions are repelled by the negatively charged walls and may accumulate inside the plasma volume. Under certain conditions, the concentration of negative ions n_n can become comparable to or even significantly exceed the free-electron concentration [9,10,38–41]. This substantially affects the transport of electrons and positive ions toward the walls, thereby reducing the ambipolar electric field strength. William B. Thompson [42] was the first to investigate ambipolar diffusion in electronegative plasma consisting of electrons, positive ions, and negative ions. He demonstrated that, in contrast to electropositive plasma, the ambipolar diffusion coefficients become different for each charged species. Further studies of ambipolar diffusion in electronegative plasmas were reported, for example, in Refs. [43–47]. These works showed that the accumulation of negative ions may not only substantially reduce the ambipolar electric field strength, but may even cause a transition from ambipolar diffusion back to free diffusion, since the ambipolar diffusion coefficients of the charged species approach their corresponding free-diffusion coefficients [47].

Nanoparticles introduced into plasma from an external reservoir or formed in situ due to electrode sputtering [48–53] or plasma-chemical processes [54–60] also capture free electrons and may therefore be regarded as very heavy negative ions. Ambipolar diffusion in plasma consisting of electrons, positive ions, and negatively charged nanoparticles has been investigated numerically in Refs. [61–63], while an analytical model was developed in Ref. [64]. In contrast to the numerical studies [61–63], which provided results only for specific plasma conditions, Ref. [64] derived convenient analytical expressions for the ambipolar diffusion coefficients of each charged species and for the ambipolar electric field strength. It was shown that a high nanoparticle concentration, and consequently strong electron losses due to electron attachment to nanoparticle surfaces, may reduce the ambipolar electric field strength to zero.

It should also be noted that technological gases in which nanoparticles are formed through volumetric plasma polymerization are often simultaneously electronegative. For example, in acetylene plasma, H^-, C_2H^- and heavier negative ions can be generated [25–27]. The C_2H^- ions may cluster with acetylene molecules during collisions, eventually leading to nanoparticle formation [65]. Therefore, acetylene plasma simultaneously contains not only electrons and positive ions, but also negative ions and nanoparticles.

The aim of the present work is to develop an analytical model for such a complex plasma system, determine the conditions under which the ambipolar electric field reverses direction, and experimentally verify this phenomenon.

1. DESCRIPTION OF THE ANALYTICAL MODEL

For a four-component plasma consisting of one species of positive ions, electrons, negative ions, and negatively charged nanoparticles, the particle flux equations can be written in the following form:

$$\Gamma_+ = -D_+ \cdot \nabla n_+ + \mu_+ n_+ E\,, \tag{1}$$

$$\Gamma_e = -D_e \cdot \nabla n_e - \mu_e n_e E\,, \tag{2}$$

$$\Gamma_n = -D_n \cdot \nabla n_n - \mu_n n_n E\,, \tag{3}$$

$$\Gamma_p = -D_p \cdot \nabla n_p - \mu_p n_p E\,, \tag{4}$$

where D denotes the free diffusion coefficients, μ the mobilities, and n the concentrations of the charged species listed above. The subscripts "e", "+", "n", and "p" correspond to electrons, positive ions, negative ions, and negatively charged nanoparticles, respectively. Owing to the formation of a space charge, an ambipolar electric field arises, whose strength is denoted by E.

In quasineutral plasma, the total concentration of positive charges must equal the total concentration of negatively charged species:

$$n_+ = n_e + n_n + n_p \cdot Z_p\,, \tag{5}$$

Here it is taken into account that a nanoparticle may collect not only one but several electrons. The number of electrons attached to a single nanoparticle is denoted by Z_p. Consequently, the product $n_p \cdot Z_p$ represents the total number of electrons attached to nanoparticles within a unit volume of 1 cm^{-3}.

Furthermore, to maintain plasma quasineutrality, the flux of positive ions must balance the total flux of negatively charged species:

$$\Gamma_+ = \Gamma_e + \Gamma_n + \Gamma_p \cdot Z_p\,. \tag{6}$$

Let us introduce the dimensionless parameters = np/ne and = nn/ne, which represent the relative concentrations of nanoparticles and negative ions, respectively, normalized to the electron concentration. We also define $\gamma = T_e/T_+ = T_e/T_n$ and $\tau = T_e/T_p$, where T_e is the electron temperature, $T_+ = T_n$ are the temperatures of positive and negative ions (assumed equal), and T_p is the nanoparticle temperature.

Substituting the flux expressions (1)–(4) into Eq. (6), and taking into account the quasineutrality condition (5), the ambipolar electric field E can be eliminated, yielding:

$$\Gamma_+ = -D_{a+} \cdot \nabla n_+ , \tag{7}$$

$$\Gamma_e = -D_{ae} \cdot \nabla n_e , \tag{8}$$

$$\Gamma_n = -D_{an} \cdot \nabla n_n , \tag{9}$$

$$\Gamma_p = -D_{ap} \cdot \nabla n_p . \tag{10}$$

These equations contain the ambipolar diffusion coefficients for each charged species:

$$D_{a+} = D_+ \cdot \frac{\gamma + 2\alpha\gamma + \gamma\cdot\delta\cdot Z_p + 1 + \delta\cdot\tau\cdot Z_p}{1 + \alpha\gamma + \delta\cdot\tau\cdot Z_p} \cdot \frac{1 + \alpha\cdot(\mu_n/\mu_e) + \delta\cdot Z_p\cdot(\mu_p/\mu_e)}{(1+\alpha+\delta\cdot Z_p)\cdot(\mu_+/\mu_e) + \alpha\cdot(\mu_n/\mu_e) + \delta\cdot Z_p\cdot(\mu_p/\mu_e) + 1}, \tag{11}$$

$$D_{ae} = D_+ \cdot \frac{\gamma + 2\alpha\gamma + \gamma\cdot\delta\cdot Z_p + 1 + \delta\cdot\tau\cdot Z_p}{(1+\alpha+\delta\cdot Z_p)\cdot(\mu_+/\mu_e) + \alpha\cdot(\mu_n/\mu_e) + \delta\cdot Z_p\cdot(\mu_p/\mu_e) + 1}. \tag{12}$$

$$D_{an} = D_+ \cdot \frac{\mu_n}{\mu_e} \cdot \frac{\gamma + 2\alpha\gamma + \gamma\cdot\delta\cdot Z_p + 1 + \delta\cdot\tau\cdot Z_p}{(1+\alpha+\delta\cdot Z_p)\cdot(\mu_+/\mu_e) + \alpha\cdot(\mu_n/\mu_e) + \delta\cdot Z_p\cdot(\mu_p/\mu_e) + 1}. \tag{13}$$

$$D_{ap} = D_+ \cdot \frac{1}{\tau} \cdot \frac{\mu_p}{\mu_e} \frac{\gamma + 2\alpha\gamma + \gamma\cdot\delta\cdot Z_p + 1 + \delta\cdot\tau\cdot Z_p}{(1+\alpha+\delta\cdot Z_p)\cdot(\mu_+/\mu_e) + \alpha\cdot(\mu_n/\mu_e) + \delta\cdot Z_p\cdot(\mu_p/\mu_e) + 1} \tag{14}$$

By equating the expressions for the positive-ion fluxes in Eqs. (1) and (7) (or similarly Eqs. (2) and (8), etc.), and using the Einstein relation $D_+/\mu_+ = k\cdot T_+/e$ where k is the Boltzmann constant and e is the elementary charge, the following expression for the ambipolar electric field strength can be derived:

$$E_{Amb.Nano} = \frac{D_+ - D_{a+}}{\mu_+ n_+} \cdot \nabla n_+ = \frac{D_+}{\mu_+} \cdot \left(1 - \frac{D_{a+}}{D_+}\right) \cdot \frac{\nabla n_+}{n_+} = T_+ \cdot \left(1 - \frac{D_{a+}}{D_+}\right) \cdot \frac{\nabla n_+}{n_+} . \tag{15}$$

Taking Eq. (11) into account, Eq. (15) can be rewritten as

$$E_{Amb.Nano} = \frac{kT_+}{e} \cdot \frac{(1+\alpha+\delta\cdot Z_p)\cdot\left[(1+\alpha\cdot\gamma+\delta\cdot\tau\cdot Z_p)\cdot(\mu_+/\mu_e) - \alpha\cdot\gamma\cdot(\mu_n/\mu_e) - \delta\cdot Z_p\cdot\gamma\cdot(\mu_p/\mu_e) - \gamma\right]}{(1+\alpha\cdot\gamma+\delta\cdot\tau\cdot Z_p)\cdot\left[(1+\alpha+\delta\cdot Z_p)\cdot(\mu_+/\mu_e) + \alpha\cdot\gamma\cdot(\mu_n/\mu_e) + \delta\cdot Z_p\cdot(\mu_p/\mu_e) + 1\right]} \cdot \frac{\nabla n_+}{n_+} \tag{16}$$

For electropositive plasma consisting only of electrons and positive ions, Eq. (16) reduces to the well-known expression for the ambipolar electric field [66–68]:

$$E_{Amb} = \frac{D_+ - D_e}{\mu_+ + \mu_e} \cdot \frac{\nabla n}{n} . \tag{17}$$

Next, let us determine the floating potential φ_s acquired by a nanoparticle of radius a immersed in plasma and collecting electrons, positive ions, and negative ions with masses m_e, M_+ та M_n, respectively. This will allow us to determine the nanoparticle charge $Q = e\cdot Z_p$ and subsequently evaluate the ambipolar electric field strength using Eq. (16).

The currents of charged particles to the nanoparticle surface can be written as [69]:

$$I_+ = 4\pi a^2 e \cdot \frac{n_+}{4} \cdot \left(\frac{8kT_+}{\pi M_+}\right)^{1/2} \cdot \left(1 - \frac{e\varphi_s}{kT_+}\right), \tag{18}$$

$$I_e = 4\pi a^2 e \cdot \frac{n_e}{4} \cdot \left(\frac{8kT_e}{\pi m_e}\right)^{1/2} \cdot \exp\left(\frac{e\varphi_s}{kT_e}\right), \tag{19}$$

$$I_n = 4\pi a^2 e \cdot \frac{n_n}{4} \cdot \left(\frac{8kT_n}{\pi M_n}\right)^{1/2} \cdot \exp\left(\frac{e\varphi_s}{kT_n}\right). \tag{20}$$

Since nanoparticles are electrically isolated, they acquire a floating potential such that the total current to their surface is zero:

$$I_+ = I_e + I_n. \tag{21}$$

Using Eqs. (18)–(21) together with the quasineutrality condition (5), we obtain the following equation for the floating potential:

$$\left(1 + \alpha + \delta \cdot Z_p\right) \cdot \left(\frac{T_+}{T_e} \cdot \frac{m_e}{M_+}\right)^{1/2} \cdot \left(1 - \frac{e\varphi_s}{kT_+}\right) - \exp\left(\frac{e\varphi_s}{kT_e}\right) - \alpha \cdot \left(\frac{T_n}{T_e} \cdot \frac{m_e}{M_n}\right)^{1/2} \cdot \exp\left(\frac{e\varphi_s}{kT_n}\right) = 0. \tag{22}$$

Usually, the nanoparticle floating potential relative to the plasma is determined only from the balance between positive-ion and electron currents to the particle surface. However, at sufficiently high negative-ion concentrations (large α), the free-electron concentration may become very low, leading to a substantial reduction in the electron current to the nanoparticle surface. Therefore, in Eqs. (21) and (22), the contribution of the negative-ion current to the nanoparticle surface has also been taken into account. Moreover, the depletion of free electrons due to their attachment to nanoparticles significantly affects plasma quasineutrality, which is reflected in the first term of Eq. (22).

As noted above, each nanoparticle collects Z_p electrons. If a nanoparticle is placed in plasma characterized by a Debye length λ_D, its charge Q is given by [69–77]:

$$Q = 4 \cdot \pi \cdot \varepsilon_0 \cdot a \cdot \left(1 + \frac{a}{\lambda_D}\right) \cdot \varphi_s, \tag{23}$$

where $\varepsilon_0 = 8.85 \cdot 10^{-12}$ F/m is the vacuum permittivity.

The Debye length can be estimated as [66]

$$\lambda_D = 742 \cdot \left(\frac{T_e\,[eV]}{n_e\,[cm^{-3}]}\right)^{1/2} [\text{cm}] \tag{24}$$

For example, for an electron temperature of 1 eV and an electron concentration of 10^{10} cm^{-3}, one obtains $\lambda_D = 74$ μm. Since nanoparticles in plasma typically have sizes of several tens to hundreds of nanometers, Eq. (23) can be simplified to

$$Q = 4 \cdot \pi \cdot \varepsilon_0 \cdot a \cdot \varphi_s. \tag{25}$$

Taking into account that $Q = e \cdot Z_p$, substituting Eq. (25) into Eq. (22) yields the final equation for the nanoparticle potential:

$$\left(1 + \alpha + \delta \cdot \frac{4 \cdot \pi \cdot \varepsilon_0 \cdot a \cdot \varphi_s}{e}\right) \cdot \left(\frac{T_+}{T_e} \cdot \frac{m_e}{M_+}\right)^{\frac{1}{2}} \left(1 - \frac{e\varphi_s}{kT_+}\right) - \exp\left(\frac{e\varphi_s}{kT_e}\right) - \alpha \left(\frac{T_n}{T_e} \cdot \frac{m_e}{M_n}\right)^{1/2} \exp\left(\frac{e\varphi_s}{kT_n}\right) = 0. \tag{26}$$

The nanoparticle potential φ_s, obtained for fixed values of α, δ, and charged-particle temperatures using Eq. (26), is substituted into Eq. (25) to determine the nanoparticle charge Z_p. Examples of the calculated nanoparticle potentials and charges are presented in Fig. 1 and Fig. 2, respectively.

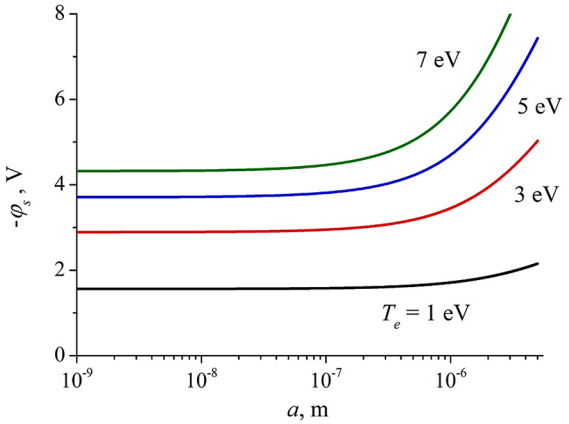

Figure 1. Dependence of the negative floating potential acquired by a nanoparticle in plasma on the nanoparticle radius a, for different electron temperatures T_e, in the absence of negative ions ($\alpha = 0$)

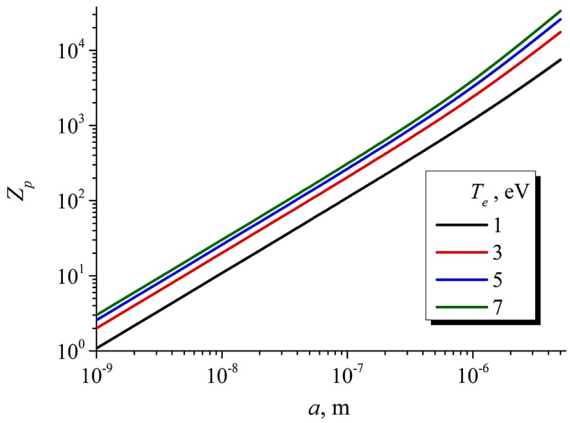

Figure 2. Dependence of the number of electrons attached to a nanoparticle in plasma on the nanoparticle radius a, for different electron temperatures T_e, in the absence of negative ions ($\alpha = 0$)

Figures 1 and 2 show that both the nanoparticle potential and charge increase with increasing electron temperature due to enhanced losses of free electrons to nanoparticle surfaces. Nanoparticle size also plays an important role. For radii $a < 100$ nm, the floating potential increases relatively slowly with increasing a, while the number of electrons attached to a nanoparticle is approximately proportional to its radius. However, for larger nanoparticles $a > 100$ nm, the rates of increase of both the potential and the charge become substantially higher.

Next, Eq. (16) is used to determine the ambipolar electric field strength. Here, our interest is focused on the average ambipolar electric field over the tube radius R, rather than on its radial distribution. An expression for the average ambipolar field in a two-component plasma (electrons and positive ions) is given, for example, in the Raizer's book [66]. Equation (16), as well as its simplified form (17), contains the factor $\nabla n_+/n_+$, which depends on the radial distribution of the positive-ion density.

To estimate this factor, Raizer assumed that the actual radial distribution of positive ions could be approximated by a straight line decreasing from its maximum value at the discharge center to zero at the tube wall of radius R. In this approximation, $\nabla n_+/n_+ \approx -1/R$.

A more realistic description of the plasma density profile often employs the zeroth-order Bessel function $n_+(r) = n_+(0)\cdot J_0(2.405\cdot r/R)$, where J_0 equals unity at the discharge axis ($r = 0$) and reaches its first root at the tube wall ($r = R$). In this case, the factor $\nabla n_+/n_+$ changes relatively weakly over most of the discharge radius, varying from zero at the axis to approximately -2 at $r = 0.8\cdot R$, and diverging rapidly to $-\infty$ only very close to the wall. Therefore, $\nabla n_+/n_+$ generally remains negative and is not directly responsible for a possible reversal of the ambipolar electric field.

However, in Eq. (16), the factor $\nabla n_+/n_+$ is multiplied by another term whose numerator may change sign depending on the parameters α, δ, γ, Z_p, and the mobility ratios of the charged species. This issue will be analyzed in more detail below. At this stage, it is sufficient to conclude that the conditions for ambipolar field reversal can be investigated using the average ambipolar field approximation with $\nabla n_+/n_+ \approx -1/R$. The average ambipolar electric field strength and the ambipolar diffusion coefficients of the charged species are important, for example, for the development of global plasma models and one-dimensional models of the positive column in dc glow discharges.

It should be noted that the calculations were performed for an acetylene plasma generated in a discharge tube with an inner radius of $R = 2.8$ cm.

The mobilities of positive and negative ions in acetylene were obtained from the analysis of experimental data reported in Ref. [78]: $\mu_+ = 1.414\cdot 10^3$ cm^2/(V·sec), $\mu_n = 1.179\cdot 10^3$ cm^2/(V·sec). The electron mobility μ_e was estimated from measured electron drift velocities in acetylene reported in Ref. [79]: $\mu_e = 2\cdot 10^5$ cm^2/(V·sec).

Let us now determine the mobility of charged nanoparticles. It can be evaluated using the expression

$$\mu_p = \frac{e\cdot Z_p}{M_p\cdot \nu_{pm}}. \tag{27}$$

As noted above, the product $e\cdot Z_p$ corresponds to the charge carried by the electrons attached to the nanoparticle. The nanoparticle collision cross section is assumed to be $\sigma = \pi\cdot a^2$ while the collision frequency between gas molecules and nanoparticles is

$$\nu_{pm} = N_{C2H2}\cdot \bar{V}_p\cdot \sigma, \tag{28}$$

where N_{C2H2} is the concentration of acetylene molecules in the discharge plasma,

$$\bar{V}_p = \left(\frac{8\cdot k\cdot T_p}{\pi\cdot M_p}\right)^{1/2}. \tag{29}$$

The nanoparticle mass can be estimated as

$$M_p = \frac{4}{3}\pi\cdot a^3\cdot \rho. \tag{30}$$

The nanoparticle material density ρ is also required. We assume that plasma polymerization processes occurring both on the chamber walls and within the plasma volume produce polymer materials (films and nanoparticles, respectively) of approximately the same density. The authors of Ref. [80] deposited polymer films from acetylene plasma and reported a density of 0.4 g/cm^{-3}, whereas Ref. [81] obtained a value of 0.6 g/cm^{-3}. Therefore, an average value of $\rho = 0.5$ g/cm^{-3} was used in the present calculations.

Substituting Eqs. (28)–(30) into Eq. (27) yields

$$\mu_p = \frac{3}{4\pi}\cdot\frac{e\cdot Z_p}{N_{C2H2}}\cdot\frac{\left(6kT_p\right)^{-1/2}}{a^{7/2}\cdot\rho^{1/2}}. \tag{31}$$

The calculated mobilities of nanoparticles of different sizes are presented in Fig. 3. Since the nanoparticle mobility μ_p is inversely proportional to $a^{7/2}$, a rapid decrease in μ_p is observed with increasing nanoparticle size.

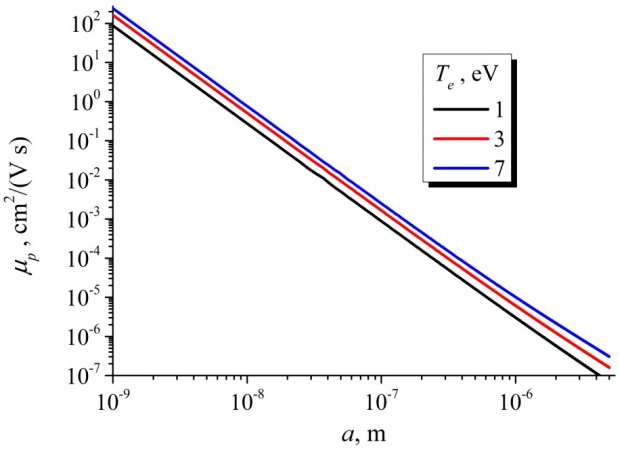

Figure 3. Dependence of nanoparticle mobility on nanoparticle radius for different electron temperatures

2. ANALYSIS OF THE AMBIPOLAR DIFFUSION COEFFICIENTS

Equations (12)–(14) for the ambipolar diffusion coefficients can be rewritten in a form more convenient for analysis:

$$D_{ae} = \frac{D_e}{\gamma}\frac{\mu_+}{\mu_e}\cdot\frac{\gamma+2\alpha\gamma+\gamma\cdot\delta\cdot Z_p+1+\delta\cdot\tau\cdot Z_p}{\left(1+\alpha+\delta\cdot Z_p\right)\cdot\left(\mu_+/\mu_e\right)+\alpha\cdot\left(\mu_n/\mu_e\right)+\delta\cdot Z_p\cdot\left(\mu_p/\mu_e\right)+1}, \tag{32}$$

$$D_{an} = \frac{D_n}{\gamma}\frac{\mu_+}{\mu_e}\cdot\frac{\gamma+2\alpha\gamma+\gamma\cdot\delta\cdot Z_p+1+\delta\cdot\tau\cdot Z_p}{\left(1+\alpha+\delta\cdot Z_p\right)\cdot\left(\mu_+/\mu_e\right)+\alpha\cdot\left(\mu_n/\mu_e\right)+\delta\cdot Z_p\cdot\left(\mu_p/\mu_e\right)+1}, \tag{33}$$

$$D_{ap} = \frac{D_p}{\gamma}\frac{\mu_+}{\mu_e}\cdot\frac{\gamma+2\alpha\gamma+\gamma\cdot\delta\cdot Z_p+1+\delta\cdot\tau\cdot Z_p}{\left(1+\alpha+\delta\cdot Z_p\right)\cdot\left(\mu_+/\mu_e\right)+\alpha\cdot\left(\mu_n/\mu_e\right)+\delta\cdot Z_p\cdot\left(\mu_p/\mu_e\right)+1}. \tag{34}$$

In Eqs. (11)–(14), all coefficients were expressed through the free diffusion coefficient of positive ions D_+. In contrast, Eqs. (32)–(34) express the ambipolar diffusion coefficients of each charged species through their own free diffusion coefficients. This representation makes it possible to analyze their behavior over a wide range of the parameters α, δ, and charged-particle temperatures.

First, let us consider a plasma containing electrons, positive ions, and negative ions, but without nanoparticles ($\delta = 0$). Using Eqs. (11), (32), and (33), the ambipolar diffusion coefficients for the charged species were calculated over a wide range of the relative negative-ion concentration α. The results are presented in Fig. 4.

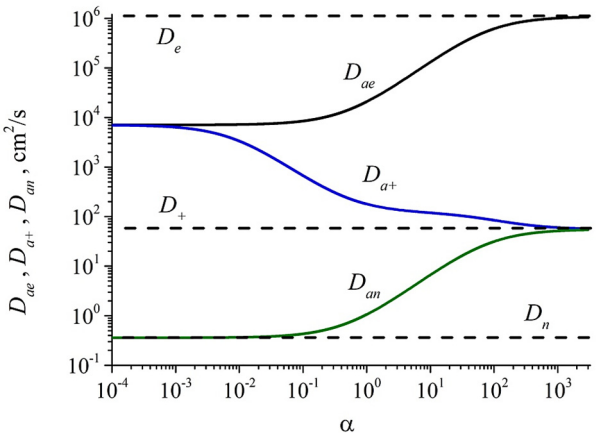

Figure 4. Dependence of the ambipolar diffusion coefficients of electrons D_{ae}, positive ions D_{a+}, and negative ions D_{an} on the relative concentration of negative ions α in the absence of nanoparticles ($\delta = 0$). Electron temperature $T_e = 5$ eV

Figure 4 shows that at very low relative concentrations of negative ions, $\alpha < 10^{-3}$, the ambipolar diffusion coefficients of electrons and positive ions coincide, $D_{ae} = D_{a+}$. In this case, the plasma effectively behaves as a two-component plasma consisting only of electrons and positive ions. For $\alpha = 0$, Eqs. (11) and (12) reduce to the classical ambipolar diffusion coefficient D_a [66–68]:

$$D_{ae} = D_{a+} \approx D_+ \frac{\gamma+1}{(\mu_+/\mu_e)+1} = \frac{D_+ \cdot \mu_e + D_e \cdot \mu_+}{\mu_e + \mu_+} = D_a \tag{35}$$

Furthermore, for small α and large $\gamma >> 1$, Eq. (33) yields $D_{an} \approx D_n \cdot (\mu_+/\mu_e) << D_n$. Thus, a small amount of negative ions added to an electron–ion plasma has almost no effect on the ambipolar diffusion process itself, while the negative ions remain effectively confined within the plasma due to their extremely small ambipolar diffusion coefficient.

However, the situation changes rapidly as the relative concentration of negative ions increases. The ambipolar diffusion coefficients of electrons D_{ae} and negative ions D_{an} increase, whereas the coefficient for positive ions D_{a+} decreases. At $\alpha > 100$, diffusion ceases to be ambipolar because $D_{ae} \to D_e$, $D_{a+} \to D_+$, $D_{an} \to D_n$. This means that charged particles of different species no longer significantly affect each other's transport. The loss of a small number of electrons from the plasma volume does not noticeably violate plasma quasineutrality; therefore, charge separation and the ambipolar electric field do not develop. Such a conclusion for strongly electronegative plasma at large α was previously reported in Ref. [47]. The present results demonstrate that the derived expressions for the ambipolar diffusion coefficients in four-component plasma, Eqs. (11) and (32)–(34), are fully consistent with previously established results for simpler plasma compositions.

Let us now consider a plasma containing electrons, positive ions, a small amount of negative ions with relative concentration $\alpha = 10^{-4}$, and charged nanoparticles. The calculated dependences of the ambipolar diffusion coefficients on the relative nanoparticle concentration δ are shown in Fig. 5a. Since the quantity of greater physical interest is not the nanoparticle concentration itself, but rather the losses of free electrons due to attachment to nanoparticles, the diffusion coefficients are also presented as functions of the product $\delta \cdot Z_p$ in Fig. 5b. For these calculations, it was determined beforehand that for an electron temperature of 5 eV and nanoparticle radius 100 nm, each nanoparticle acquires approximately $Z_p \approx 265$ electrons.

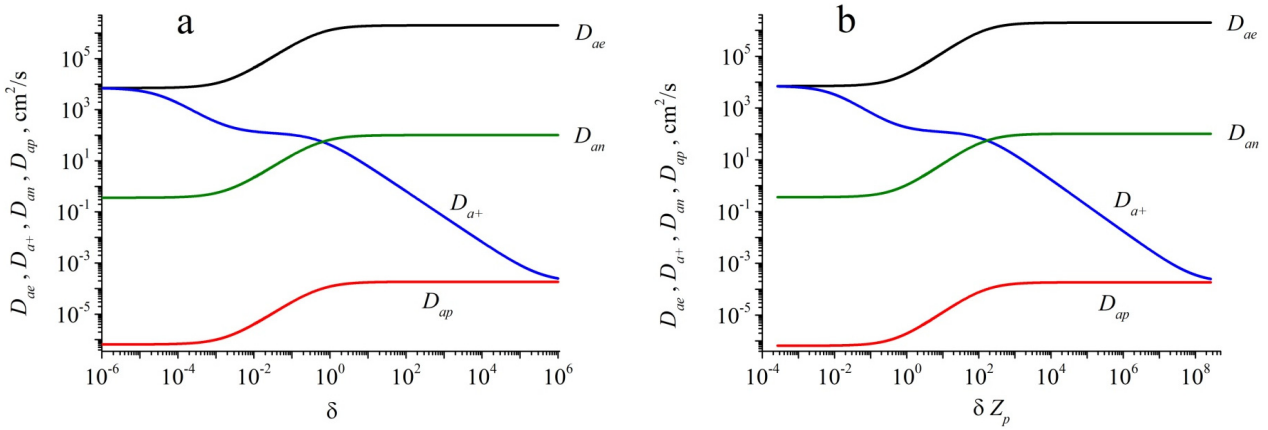

Figure 5. Dependence of the ambipolar diffusion coefficients of electrons D_{ae}, positive ions D_{a+}, negative ions D_{an}, and nanoparticles D_{ap} on the relative nanoparticle concentration δ (a) and on the product $\delta \cdot Z_p$ (b) at low relative concentration of negative ions ($\alpha = 10^{-4}$). Nanoparticle radius $a = 100$ nm, electron temperature $T_e = 5$ eV

Figure 5 indicates that the diffusion process remains essentially ambipolar, similarly to a two-component electron–ion plasma, only at very low nanoparticle concentrations, $\delta < 10^{-5}$. Under these conditions, the ambipolar diffusion coefficient of nanoparticles is extremely small, $D_{ap} \approx D_p \cdot (\mu_+/\mu_e) << D_p$. Thus, negatively charged nanoparticles, similarly to negative ions introduced in small concentration, are efficiently confined within the plasma volume by the strong ambipolar electric field.

However, with increasing δ, the ambipolar diffusion coefficients of nanoparticles, electrons, and negative ions increase rapidly and eventually approach saturation values. For $\alpha << 1$ and $\delta >> 1$, one obtains $D_{ap} \approx 2 \cdot D_p$, $D_{ae} \approx 2 \cdot D_e$, $D_{an} \approx 2 \cdot D_n$. It should be emphasized that these coefficients at $\delta >> 1$ ($\delta \cdot Z_p >> 1$) are twice as large as the corresponding free diffusion coefficients, unlike the case without nanoparticles at large $\alpha >> 1$, where the ambipolar coefficients simply approach the free-diffusion values.

In realistic discharge plasma, however, both negative ions and nanoparticles may be present simultaneously in significant concentrations. Therefore, for the limiting case $\alpha >> 1$ and $\delta \cdot Z_p >> 1$, Eqs. (32)–(34) reduce to:

$$D_{ae} = D_e \cdot \left(1 + \frac{\delta \cdot Z_p}{2\alpha + \delta \cdot Z_p}\right), \tag{36}$$

$$D_{an} = D_n \cdot \frac{2 \cdot (\alpha + \delta \cdot Z_p)}{2\alpha + \delta \cdot Z_p}, \tag{37}$$

$$D_{ap} = D_p \cdot \frac{2 \cdot (\alpha + \delta \cdot Z_p)}{2\alpha + \delta \cdot Z_p}. \tag{38}$$

From Eq. (36), it follows that for $\delta \cdot Z_p >> \alpha$, we have $D_{ae} \approx 2 \cdot D_e$, whereas for the opposite condition $\delta \cdot Z_p << \alpha$, $D_{ae} \approx D_e$. Similarly, Eqs. (37) and (38) yield $D_{an} \approx 2 \cdot D_n$ and $D_{ap} \approx 2 \cdot D_p$, for $\delta \cdot Z_p >> \alpha$, while $D_{an} \approx D_n$ та $D_{ap} \approx D_p$ for $\delta \cdot Z_p << \alpha$.

The situation is more complicated for positive ions. Figure 5 shows that with increasing nanoparticle concentration δ, the ambipolar diffusion coefficient of positive ions initially decreases and tends to approach the coefficient for negative ions, $D_{a+} \to D_{an}$ similarly to the behavior observed in Fig. 4 for plasma without nanoparticles ($\delta = 0$). However, with further increase in δ and $\delta \cdot Z_p$, the coefficient D_{a+} decreases again and eventually approaches $D_{a+} \to D_{ap}$.

Of course, the regime $D_{a+} \approx D_{ap}$ corresponds to extremely low free-electron concentrations, when the plasma effectively consists only of positive ions and negatively charged nanoparticles. Such a situation may arise, for example, in corona discharges with low discharge current and low electron density in aerosol media ("foggy plasmas"), where fine droplets capture nearly all free electrons.

Analysis of Eq. (11) under the simultaneous conditions $\alpha >> 1$ and $\delta \cdot Z_p >> 1$ gives:

$$D_{a+} = 2D_+ \cdot \frac{\alpha + \delta \cdot Z_p \cdot (\mu_p / \mu_+)}{2\alpha + \delta \cdot Z_p}, \tag{39}$$

This expression shows that for $\delta \cdot Z_p << \alpha$ one obtains $D_{a+} \approx D_+ \approx D_n$, whereas for $\delta \cdot Z_p \cdot (\mu_p/\mu_+) >> \alpha$ the limiting relation becomes $D_{a+} \approx 2 \cdot D_p$. Thus, *the ambipolar diffusion coefficient of positive ions strongly depends on which negatively charged species dominate in the plasma*. If negative ions dominate, then at sufficiently high concentrations of electronegative species (large electron losses due to attachment to gas molecules), we have $D_{a+} \to D_n$. In plasma where electron losses due to attachment to nanoparticles dominate, the asymptotic behavior becomes $D_{a+} \to 2 \cdot D_p = D_{ap}$.

This unusual behavior of positive ions can be understood rather straightforwardly. In a two-component plasma consisting only of electrons and positive ions, both species leave the plasma region (for example, toward the discharge-tube walls) with approximately equal fluxes: $\Gamma_+ \approx \Gamma_e$. If a substantial fraction of electrons attaches to molecules and forms negative ions with $\alpha >> 1$, then the loss of a small number of free electrons is no longer critical for sustaining the discharge, and the balance condition becomes $\Gamma_+ \approx \Gamma_n$. Finally, if almost all electrons attach to nanoparticles, while the concentrations of free electrons and negative ions remain relatively small, then the positive-ion flux from the plasma must compensate the extremely small flux of heavy nanoparticles: $\Gamma_+ \approx \Gamma_p$.

The calculated dependences of the ambipolar diffusion coefficients on the product $\delta \cdot Z_p$ for a high relative concentration of negative ions, $\alpha = 100$, are shown in Fig. 6. The initially high concentration of negative ions results in relatively large ambipolar diffusion coefficients for electrons, nanoparticles, and negative ions even at low nanoparticle concentrations; these coefficients are already close to their free-diffusion values. With increasing electron losses to nanoparticles $\delta \cdot Z_p$, these coefficients increase further and approach twice their free-diffusion values. In contrast, the ambipolar diffusion coefficient of positive ions is initially close to twice its free-diffusion value, but decreases rapidly with increasing $\delta \cdot Z_p$, eventually approaching the nanoparticle ambipolar diffusion coefficient.

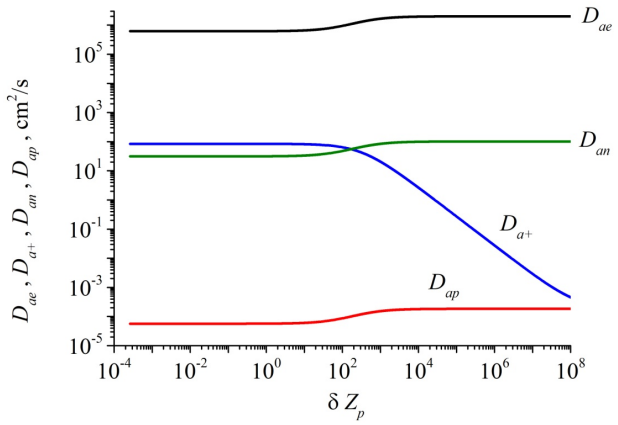

Figure 6. Dependence of the ambipolar diffusion coefficients of electrons, positive and negative ions, and nanoparticles on the product $\delta \cdot Z_p$ at relative concentration of negative ions $\alpha = 100$. Nanoparticle radius $a = 100$ nm, electron temperature $T_e = 5$ eV

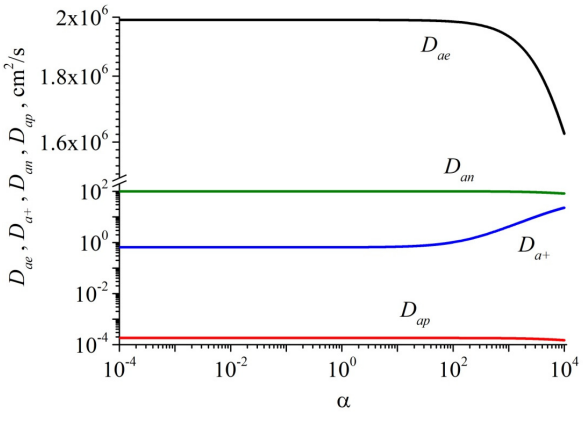

Figure 7. Dependence of the ambipolar diffusion coefficients of electrons, positive and negative ions, and nanoparticles on the relative concentration of negative ions α at $\delta = 100$. Nanoparticle radius $a = 100$ nm, electron temperature $T_e = 5$ eV

Finally, let us consider the case of plasma with a high relative concentration of nanoparticles ($\delta = 100$). The corresponding results are presented in Fig.7. At low negative-ion concentrations, the electron ambipolar diffusion coefficient D_{ae} is approximately equal to twice the free electron diffusion coefficient. However, at $\alpha > 100$, D_{ae}

decreases and approaches the free electron diffusion coefficient. The ambipolar diffusion coefficients of nanoparticles and negative ions behave similarly, decreasing from twice their free-diffusion values toward the corresponding free-diffusion coefficients. The behavior of the positive-ion ambipolar diffusion coefficient again appears unusual: initially small, it increases at $\alpha > 100$ and eventually approaches the free diffusion coefficient at very large α.

Therefore, the ambipolar diffusion process in four-component plasma is highly complex and strongly depends on the relative importance of free-electron losses due to attachment either to nanoparticles or to electronegative gas molecules forming stable negative ions. The dominant electron-loss mechanism ultimately determines the ambipolar diffusion coefficients of all charged species present in the plasma.

3. AMBIPOLAR ELECTRIC FIELD

As noted above, we are primarily interested in the average value of the ambipolar electric field strength over the discharge-tube radius. It is this field that controls the confinement of negatively charged ions and nanoparticles within the plasma volume. Therefore, we calculated its magnitude for different plasma conditions and nanoparticle sizes.

The calculated results will be compared with those for a conventional two-component plasma consisting only of electrons and positive ions. The corresponding ambipolar electric field strength E_{Amb} obtained from Eq. (17) will hereafter be referred to as the "classical" ambipolar field. For an electron temperature of 5 eV, its value is shown in Fig. 8 and is approximately equal to 1.77 V/cm. Naturally, this field does not depend on the nanoparticle radius, since Eq. (17) does not account for the possible presence of nanoparticles in plasma.

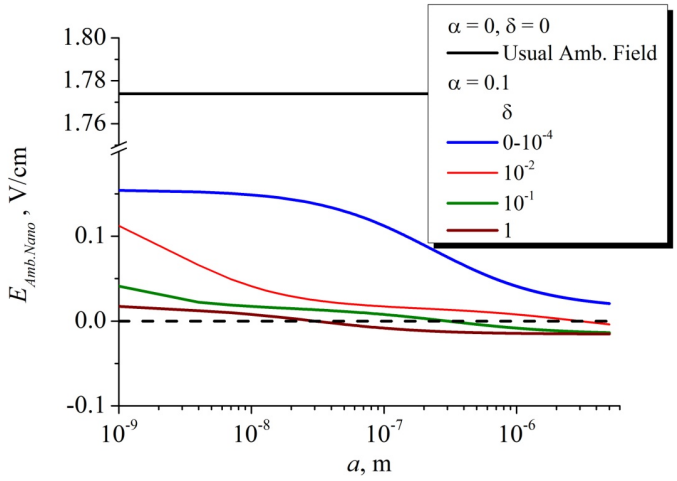

Figure 8. Dependence of the average ambipolar electric field on nanoparticle radius at $\alpha = 0.1$ for different values of the relative nanoparticle concentration δ. Electron temperature $T_e = 5$ eB

Let us now consider plasma additionally containing negative ions with a relatively low concentration $\alpha = 0.1$. This means that approximately 10% of the electrons have attached to gas molecules and formed negative ions. However, even such comparatively moderate electron losses lead to a substantial, nearly tenfold reduction in the ambipolar electric field strength (the blue curve in Fig. 8 at small nanoparticle radii). If nanoparticles are additionally introduced into the plasma and their size increases, the ambipolar electric field strength rapidly decreases and approaches zero.

Let us further increase the nanoparticle concentration in plasma. As the relative nanoparticle concentration δ increases, volumetric polymerization processes also lead to an increase in nanoparticle radius. Figure 8 shows that at sufficiently high nanoparticle concentration and sufficiently large nanoparticle size, the ambipolar electric field reaches zero and may even reverse its sign. The larger the relative nanoparticle concentration δ, the smaller the nanoparticle radius at which this sign reversal occurs.

Let us examine the behavior of the ambipolar electric field under different conditions. Figure 9 presents its dependence on the relative concentration α for different values of δ. If nanoparticles are absent from plasma ($\delta = 0$) and negative ions are present only in very small amounts ($\alpha \leq 10^{-4}$), the ambipolar field strength remains close to its "classical" value given by Eq. (17). Increasing α results in a gradual decrease in the ambipolar field strength, and at $\alpha \approx$ 850 the field reaches zero and subsequently reverses its sign as the negative-ion concentration increases further.

In the presence of nanoparticles (the curves in Fig. 9 corresponding to $\delta = 10^{-4}$, 10^{-2} and 1), increasing their concentration substantially reduces the ambipolar electric field strength. In fact, negative ions and charged nanoparticles jointly affect the field magnitude. The ambipolar field again reaches zero at sufficiently high α and then changes sign. Moreover, the higher the relative nanoparticle concentration δ, the smaller the value of α at which this occurs. For example, at $\delta = 10^{-2}$ and $\delta = 1$, the sign reversal of the ambipolar field occurs at $\alpha = 826$ and $\alpha = 796$, respectively. If the nanoparticle concentration becomes very high, for example $\delta = 100$, the ambipolar electric field remains negative over the entire α range, and the corresponding curve in Fig. 9 lies entirely below zero.

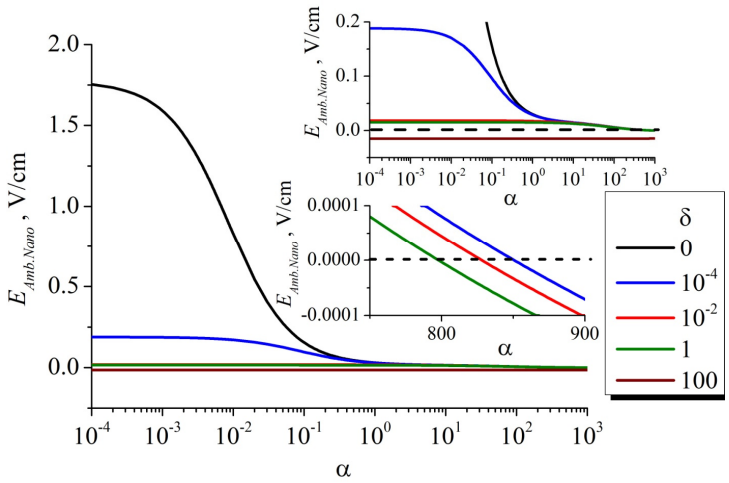

Figure 9. Dependence of the average ambipolar electric field on α for different values of the relative nanoparticle concentration δ and nanoparticle radius a = 100 nm, T_e = 5 eV

It is also instructive to consider the dependence of the average ambipolar electric field strength on the product δZ_p rather than only on the relative nanoparticle concentration δ (see Fig. 10). Since for nanoparticle radius a = 100 nm and electron temperature 5 eV, one has $Z_p \approx 265$, replacing δ with δZ_p shifts the corresponding ambipolar-field curves toward larger values along the horizontal axis.

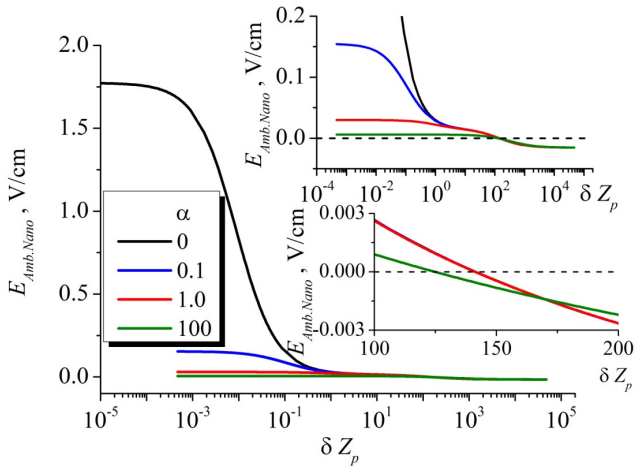

Figure 10. Dependence of the average ambipolar electric field on the product δZ_p for different values of the relative negative-ion concentration α and nanoparticle radius a = 100 nm, T_e = 5 eV

Similarly to the previous case, the ambipolar electric field decreases with increasing both the relative concentration of negative ions α and the normalized number of electrons attached to nanoparticles δZ_p. At $\alpha \leq 1$, the curves corresponding to different α practically coincide for $\delta Z_p \geq 10$, and the ambipolar field reaches zero at approximately the same value, $\delta Z_p \approx 141$. However, at higher α the sign reversal occurs earlier. For example, at $\alpha = 100$ the ambipolar field changes sign already at $\delta Z_p \approx 123$.

The reversal of the ambipolar electric field at sufficiently high concentrations of nanoparticles and negative ions indicates the appearance of conditions for the removal of their excess from plasma. In real gas-discharge plasma, the ambipolar electric field strength will likely remain close to zero or slightly negative. If an excessive number of nanoparticles and negative ions is produced, the ambipolar field will drive their excess toward the discharge-tube walls, after which the field will again approach zero. The stationary state corresponds to a zero ambipolar electric field, while the nanoparticle concentration reaches saturation.

Thus, if a sufficiently dense nanoparticle cloud is present in plasma, the ambipolar electric field inside this cloud may become nearly zero. As shown above, at high nanoparticle concentrations the ambipolar diffusion coefficients of electrons, negatively charged ions, and nanoparticles approach twice their free-diffusion values. In three-component plasma (electrons, positive ions, and negative ions), ambipolar diffusion effectively transformed into free diffusion for all charged species. However, after introducing nanoparticles into plasma, the diffusion losses of negatively charged species become additionally enhanced by a factor of two owing to their removal from the plasma volume by the electric field after it reverses its sign.

To determine the conditions for ambipolar-field sign reversal in more detail, let us analyze Eq. (16). Its denominator is a combination of positive quantities. However, the numerator contains a factor in square brackets that may become zero under the condition given by Eq. (40).

$$\left(1+\alpha\cdot\gamma+\delta\cdot\gamma\cdot Z_p\right)\cdot\left(\mu_+/\mu_e\right)-\alpha\cdot\gamma\cdot\left(\mu_n/\mu_e\right)-\delta\cdot Z_p\cdot\gamma\cdot\left(\mu_p/\mu_e\right)-\gamma=0\,. \tag{40}$$

Equation (40) can be rewritten in the following form:

$$\delta\cdot Z_p=\frac{\mu_e}{\mu_+-\mu_p}\cdot\left[1-\frac{1}{\gamma}\cdot\frac{\mu_+}{\mu_e}+\alpha\cdot\left(\frac{\mu_n}{\mu_e}-\frac{\mu_+}{\mu_e}\right)\right]. \tag{41}$$

From Eq. (41), it follows that the value of δZ_p at which the ambipolar electric field changes sign depends only weakly on the electron temperature. Since $\gamma = T_e/T_+ >> 1$ and simultaneously $\mu_+/\mu_e << 1$, the second term inside the square brackets in Eq. (41) may be neglected. Calculations show (see Fig. 11) that the dependences of δZ_p on α for different electron temperatures (from 1 eV to 10 eV) practically coincide for nanoparticle radius a = 100 nm. Since the calculations were performed for acetylene plasma, where the mobility of negative ions is lower than that of positive ions (μ_+ = 1414 cm^2/(V·s), μ_n = 1179 cm^2/(V·s)), the dependence in Fig. 11 decreases approximately linearly with increasing α.

However, some dependence on electron temperature appears for very small nanoparticles. Figure 11 shows that the curves corresponding to nanoparticle radius a = 1 nm and electron temperatures 1 eV and 5 eV differ substantially from each other. In Fig.3, we presented the calculated nanoparticle mobility μ_p, which decreases rapidly with increasing nanoparticle size. At the same time, increasing electron temperature leads to an increase in μ_p. The mobility of small nanoparticles with radii of the order of several nanometers may reach 100–200 cm^2/(V·s), corresponding to 10–20% of the positive-ion mobility. Therefore, the denominator of the factor preceding the square brackets in Eq. (41) may vary significantly in this case.

Therefore, in Fig.12 the values of δZ_p corresponding to ambipolar-field sign reversal remain nearly constant over a wide range of nanoparticle radii at fixed α, but increase noticeably for radii a < 5 nm. Figure 12 also demonstrates that δZ_p decreases with increasing relative concentration of negative ions α, as already discussed above.

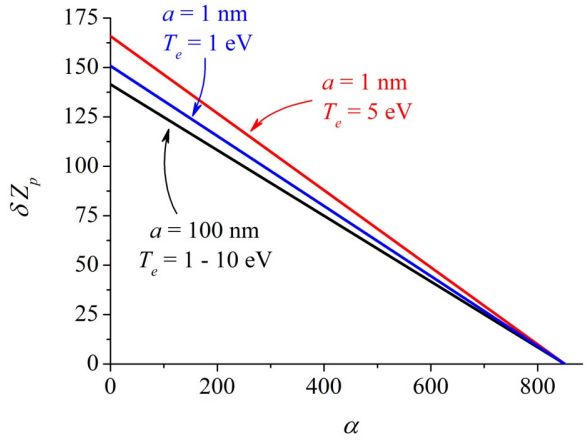

Figure 11. Dependence of the product δZ_p, at which the ambipolar electric field reaches zero, on the relative concentration of negative ions α for nanoparticle radii a = 1 nm and a = 100 nm at different electron temperatures

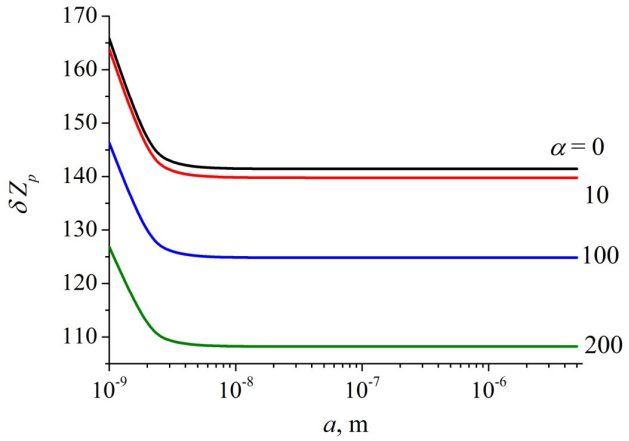

Figure 12. Dependence of the values of δZ_p corresponding to zero ambipolar electric field on nanoparticle radius for different values of the relative negative-ion concentration α at electron temperature 5 eV

If the relative concentration of negative ions is fixed at α = 100, then for nanoparticles with radii a > 10 nm the calculated values of δZ_p corresponding to different electron temperatures coincide with each other. However, for smaller nanoparticles with radii a < 10 nm, the curves corresponding to different electron temperatures diverge strongly. This means that in plasma containing very small nanoparticles with radii $a \approx 1$ nm and hot electrons, a larger relative nanoparticle concentration δ is required for ambipolar-field sign reversal than in plasma containing larger nanoparticles.

Calculations show that nanoparticles with radius 1 nm collect Z_p = 1 and Z_p = 3 electrons at electron temperatures of 1 eV and 7 eV, respectively. As follows from Fig. 13, sign reversal of the ambipolar field for such 1 nm particles requires δ = 133 at T_e = 1 eV and δ = 150/3 = 50 at T_e = 7 eV. For large nanoparticles, for example with a = 100 nm, one has $Z_p \approx 265$ and $\delta Z_p \approx 125$. Therefore, the corresponding relative concentration of such large nanoparticles is much smaller, δ = 125/265 ≈ 0,47. This means that approximately one nanoparticle with a = 100 nm is required per two free electrons for the ambipolar electric field strength to reach zero and potentially reverse its sign.

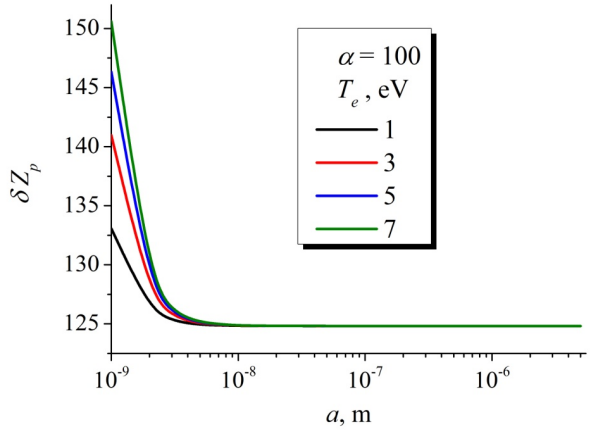

Figure 13. Dependence of the values of δZ_p corresponding to zero ambipolar electric field on nanoparticle radius at relative concentration of negative ions $\alpha = 100$ for different electron temperatures

IV. Experimental Verification

Direct experimental measurements of the radial ambipolar electric field strength in acetylene plasma using Langmuir probes and wall probes are difficult because their surfaces are rapidly covered by dielectric polymer films. In addition, the gas pressure and plasma parameters also vary with time [58,64].

However, there exists a pronounced phenomenon confirming the possibility of ambipolar-field sign reversal. Let us consider the conditions of our experiments.

The experiments were performed in a quartz discharge tube with an inner diameter of 80 mm, in the acetylene pressure range of 0.05–1 Torr, while the maximum acetylene flow rate reached 5 sccm. The distance between the flat steel electrodes was 76.2 mm. The electrodes were positioned vertically inside the tube, whereas the discharge tube itself was oriented horizontally. A DC or 20 kHz AC voltage was applied to the powered electrode (cathode).

When the electrodes are arranged horizontally inside a discharge tube or chamber, nanoparticles introduced into plasma from an external source or formed in the discharge due to volumetric polymerization are trapped near the boundary of the cathode sheath or electrode sheath by the strong electric field in these discharge regions. In contrast, the vertical arrangement of the electrodes made it possible to reveal the influence of the ambipolar electric field on nanoparticle confinement.

Here, we will not focus on the specific discharge regions where the nanoparticle cloud is formed or on the methods used for its detection. For the present discussion, it is sufficient to note the experimental observation that during discharge operation the tube walls become coated with a certain substance of particular interest. This substance appears after several tens of seconds of discharge operation in acetylene. Such behavior was observed both in dc discharges and in pulsed and high-frequency capacitive discharges. Photographs of the discharge tube with this deposited coating are shown in Figs. 14 and 15. During the discharge operation, the cathode was on the left and the anode on the right.

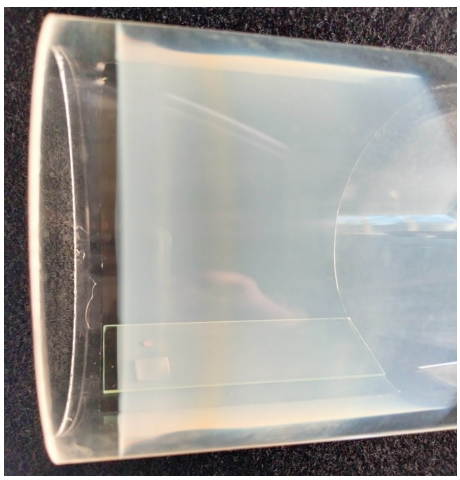

Figure 14. Photograph of the discharge tube with a deposited layer of polymer film containing nanoparticles. DC discharge. Acetylene pressure 0.5 Torr. Voltage between electrodes 1000 V, discharge current 14 mA. Film deposition time 1 min

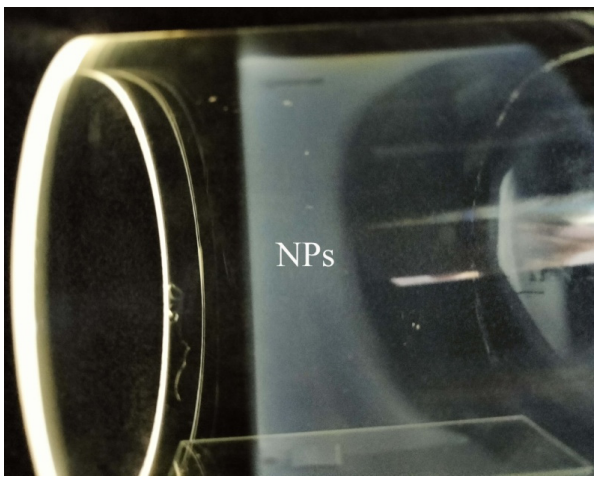

Figure 15. Photograph of the discharge tube with a deposited layer of polymer film containing nanoparticles (NPs). Bipolar pulsed discharge with frequency 20 kHz and duty cycle 50%. Acetylene pressure 0.14 Torr. Peak-to-peak voltage between electrodes 1419 V. Film deposition time 1 min

Near the cathode or powered electrode of the pulsed discharge, the cathode sheath or electrode sheath is formed, and the large voltage drop across this region expels negatively charged nanoparticles into the plasma volume. Therefore, only a thin polymer film can be deposited there. In the negative glow region, by contrast, the inner surface of the tube becomes covered with a layer of material that becomes opaque as its thickness increases.

Samples of this material were deposited onto grids for transmission electron microscopy (TEM) in a Selmi REM-125 K. The grids were positioned both at the bottom of the tube and in its upper part. Figure 16 shows a TEM image of the surface of a grid placed in the upper part of the discharge tube, recorded at a magnification of 25,000×. It can be seen that a polymer film containing a large number of embedded nanoparticles with diameters of 10–20 nm was deposited on the grid.

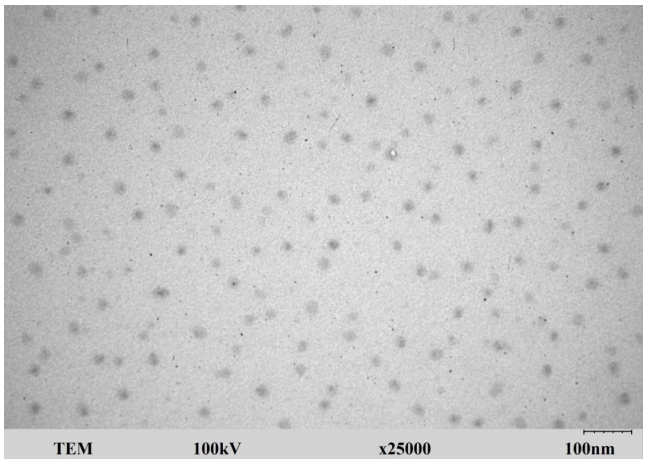

Figure 16. TEM image of the polymer film and embedded nanoparticles deposited onto the upper part of the tube from a dc discharge at acetylene pressure 0.15 Torr and deposition time 30 s. Voltage between electrodes 471 V, discharge current 1 mA

These nanoparticles were formed not on the surface itself, but inside the plasma volume. Free electrons attach to them, charging them negatively. Under ordinary conditions, the ambipolar electric field arises when a fraction of energetic free electrons escapes from plasma to the tube wall, charging it negatively. The resulting field subsequently attracts positive ions toward the wall and repels colder electrons and negatively charged nanoparticles back into the plasma volume. The Coulomb force prevents such nanoparticles from settling onto the bottom of the tube and acts against gravity. For the upper part of the tube, the same Coulomb force, together with gravity, should instead drive negatively charged nanoparticles back toward the plasma volume. Nevertheless, small nanoparticles were found embedded inside the polymer film deposited on the upper part of the tube, meaning that they must have moved against both gravitational and Coulomb forces.

However, the analytical calculations presented above demonstrated that nanoparticle accumulation in plasma leads to a substantial reduction of the ambipolar electric field strength. When the nanoparticle concentration reaches a critical value (more precisely, when the number of electrons attached to nanoparticles per unit plasma volume becomes sufficiently high), the ambipolar field reaches zero and may reverse its sign. In this case, the field begins to confine positive ions within the plasma while expelling excess negatively charged nanoparticles and negative ions from it. This mechanism is responsible for the radial ejection of nanoparticles from the plasma in all directions, including upward. It should be noted that the ion drag force, which is commonly taken into account when analyzing nanoparticle transport in plasma, is not expected to play a significant role in the present case, because the radial ambipolar electric field approaches zero and therefore does not provide substantial acceleration of positive ions.

CONCLUSIONS

In this work, the process of ambipolar diffusion in a four-component plasma consisting of electrons, positive ions, negative ions, and negatively charged nanoparticles has been investigated. An analytical model was developed based on the conditions of plasma quasineutrality and zero total current of all charged species to the discharge-tube wall. As a result, simple analytical expressions were obtained for the ambipolar diffusion coefficients of each charged species, as well as for the ambipolar electric field strength.

The derived expressions were analyzed over wide ranges of the relative concentrations of negative ions α, nanoparticles δ, the normalized concentration of electrons attached to nanoparticles δZ_p, and electron temperature. It was shown that in plasma consisting of electrons, positive ions, and negative ions, the ambipolar diffusion regime gradually transforms into free diffusion at high relative concentrations of negative ions α. In this limit, the ambipolar diffusion coefficient of electrons approaches the free electron diffusion coefficient, while the ambipolar diffusion coefficients of positive and negative ions approach their corresponding free diffusion coefficients, which are close to each other.

In plasma containing electrons, positive ions, and negatively charged nanoparticles, high nanoparticle concentrations lead to qualitatively different behavior. In this case, the ambipolar diffusion coefficient of electrons approaches twice the

free electron diffusion coefficient, whereas the diffusion flux of positive ions compensates mainly the ambipolar losses of nanoparticles. For the general four-component plasma, the behavior of the ambipolar diffusion coefficients is governed by the dominant electron-loss mechanism, namely electron attachment either to electronegative gas molecules or to nanoparticles. If electron attachment to gas molecules dominates, the ambipolar diffusion coefficients of electrons, negative ions, and nanoparticles remain close to their free diffusion coefficients. In contrast, when electron losses to nanoparticles dominate, these coefficients approach twice the corresponding free diffusion coefficients.

The behavior of the ambipolar diffusion coefficient for positive ions was found to be particularly unusual and strongly dependent on the dominant negatively charged species in the plasma. It approaches the free diffusion coefficient of negative ions under conditions of intensive negative-ion formation, whereas in a plasma dominated by electron attachment to nanoparticles, it approaches twice the free diffusion coefficient of nanoparticles.

It was further demonstrated that the accumulation of negative ions and/or negatively charged nanoparticles substantially reduces the ambipolar electric field strength. Under critical conditions, the ambipolar electric field may reach zero and even reverse its sign. A stationary plasma state corresponds to a nearly zero or slightly negative ambipolar field, which can remove excess negative ions and nanoparticles from the plasma volume.

Experimental observations performed in acetylene plasma demonstrated intensive radial removal of small nanoparticles from the plasma volume, including toward the upper part of the discharge tube against gravity. This behavior may serve as indirect evidence of ambipolar electric field reversal caused by high concentrations of negative ions and charged nanoparticles.

ORCID

V. Lisovskiy, https://orcid.org/0000-0002-6339-4516; **S. Dudin,** https://orcid.org/0000-0001-9161-4654;
S. Bogatyrenko, https://orcid.org/0000-0002-6044-6886; **S. Rezunenko,** https://orcid.org/0009-0001-5871-495X
V. Yegorenkov, https://orcid.org/0000-0002-7252-3711

REFERENCES

[1] A. Fridman, and G. Friedman, *Plasma Medicine*, (John Wiley, Chichester. 2013).
[2] M. Domonkos, P. Tichá, J. Trejbal, and P. Demo, Appl. Sci. **11**, 4809 (2021). https://doi.org/10.3390/app11114809
[3] C. E. Luchian, C. Lungoci, M.-A. Ciolan, C.-M. Rimbu, L. D. Miron, and I. Motrescu, Appl. Sci. **15**, 10366 (2025). https://doi.org/10.3390/app151910366
[4] P. Attri, K. Ishikawa, T. Okumura, K. Koga, and M. Shiratani, Processes **8**, 1002 (2020). https://doi.org/10.3390/pr8081002
[5] N. Puač, M. Gherardi, and M. Shiratani, Plasma Processes and Polymers, **15**, 1700174 (2018). https://doi.org/10.1002/ppap.201700174
[6] N.N. Misra, Oliver Schlüter, and P.J. Cullen, editors, *Cold Plasma in Food and Agriculture: Fundamentals and Applications*, (Academic Press, London, 2016). https://doi.org/10.1016/C2014-0-00009-3
[7] W. Schottky, Physikalische Zeitschrift **25**, 342 (1924).
[8] W. Schottky, and J. Issendorff, Zeitschrift für Physik **31**, 163 (1925). https://doi.org/10.1007/BF02980570
[9] V. Lisovskiy, S. Dudin, and V. Yegorenkov, Phys. Scr. **98**, 106101 (2023). https://doi.org/10.1088/1402-4896/acf89c
[10] V. Lisovskiy, J.-P. Booth, J. Jolly, S. Martins, K. Landry, D. Douai, V. Cassagne, and V. Yegorenkov, J. Phys. D: Appl. Phys. **40**, 6989 (2007). https://doi.org/10.1088/0022-3727/40/22/020
[11] N. R. Behera, A. K. Kanakati, S. Barik, S. Dutta, and G. Aravind, J. Chem. Phys. **163**, 024322 (2025). https://doi.org/10.1063/5.0278243
[12] B. Naik, Sh. Sharma, R. Narayanan, D. Sahu, M. Bandyopadhyay, A. Chakraborty, M. Singh, R. D. Tarey, and A. Ganguli, J. Instrumentation, **20**, C09003 (2025). https://doi.org/10.1088/1748-0221/20/09/C09003
[13] Z. E. Ankouri, M. El Bojaddaini, M. E. Kaouini, A. Missaoui, and H. Chatei, Contributions to Plasma Physics, **65**, e70058 (2025). https://doi.org/10.1002/ctpp.70058
[14] A. Paul, S. Melanson, T. Junginger, and M. Dehnel, J. Phys. Confer. Series, **2743**, 012083 (2024). https://doi.org/10.1088/1742-6596/2743/1/012083
[15] A. Paul, S. Melanson, T. Junginger, and M. Dehnel, J. Instrumentation, **19**, C05053 (2024). https://doi.org/10.1088/1748-0221/19/05/C05053
[16] I. Sereda, Y. Hrechko, M. Azarenkov, and K. Sereda, Intern. J. Hydrogen Energy, **109**, 1321 (2025). https://doi.org/10.1016/j.ijhydene.2025.02.222
[17] I. Sereda, Y. Hrechko, and M. Azarenkov, Phys. Plasmas, **31**, 053516 (2024). https://doi.org/10.1063/5.0202579
[18] I. Sereda, Y. Hrechko, I. Babenko, and M. Azarenkov, Vacuum, **200**, 111006 (2022). https://doi.org/10.1016/j.vacuum.2022.111006
[19] C. Poggi, A. Pimazzoni, E. Sartori, and G. Serianni, Nuclear Fusion, **65**, 026064 (2025). https://doi.org/10.1088/1741-4326/adabf9
[20] M. Bacal, editor, *Physics and Applications of Hydrogen Negative Ion Sources* (Springer, Cham, Switzerland, 2023). https://doi.org/10.1007/978-3-031-21476-9
[21] V. Dudnikov, *Development and Applications of Negative Ion Sources*, (Springer, Cham, Switzerland, 2023). https://doi.org/10.1007/978-3-031-28408-3
[22] V. Lisovskiy, S. Dudin, A. Shakhnazarian, P. Platonov, and V. Yegorenkov, East European Journal of Physics, (3), 172 (2024). https://doi.org/10.26565/2312-4334-2024-3-17
[23] S. V. Dudin, S. D. Yakovin, and A. V. Zykov, East European Journal of Physics **3**, 606 (2023). https://doi.org/10.26565/2312-4334-2023-3-72
[24] V. O. Litvinov, I. I. Okseniuk, D. I. Shevchenko, and V. V. Bobkov, East European Journal of Physics **3**, 10 (2023). https://doi.org/10.26565/2312-4334-2023-3-01

[25] M. Jiménez-Redondo, I. Tanarro, and V.J. Herrero, Plasma Sources Sci. Technol. **31**, 065003 (2022). https://doi.org/10.1088/1361-6595/ac70f8
[26] T. Wang, Sh. Rauf, N. Friedrichs, I. Korolov, J. Kenney, and J. Schulze, Phys. Plasmas, **33**, 023501 (2026). https://doi.org/10.1063/5.0300388
[27] I. Tanarro, R. J. Peláez, and V. J. Herrero, Plasma Physics and Controlled Fusion, **67**, 035014 (2025). https://doi.org/10.1088/1361-6587/adb17b
[28] K. Kalita, R. Moulick, and B. Saikia, Phys. Plasmas, **32**, 62105 (2025). https://doi.org/10.1063/5.0267438
[29] V. Lisovskiy, J.-P. Booth, K. Landry, D. Douai, V. Cassagne, and V. Yegorenkov, J. Phys. D: Appl. Phys. **40**, 6631 (2007). https://doi.org/10.1088/0022-3727/40/21/023
[30] V. Lisovskiy, J.-P. Booth, K. Landry, D. Douai, V. Cassagne, and V. Yegorenkov, Plasma Sources Sci. Technol. **17**, 025002 (2008). https://doi.org/10.1088/0963-0252/17/2/025002
[31] E. Baratte, L. Kuijpers, T. Silva, V. Guerra, M. C. M. van de Sanden, J.-P. Booth, and O. Guaitella, Plasma Sources Sci. Technol. **35**, 015009 (2026). https://doi.org/10.1088/1361-6595/ae24a9
[32] P. Viegas, B. Berdugo, and V. Guerra. Plasma Chemistry and Plasma Processing, **46**, 22 (2026). https://doi.org/10.1007/s11090-025-10607-7
[33] R. Masheyeva, M. Vass, M. Myrzaly, Ch.-B. Tian, K. Dzhumagulova, J. Schulze, Z. Donkó, and P. Hartmann, Plasma Sources Sci. Technol. **34**, 045017 (2025). https://doi.org/10.1088/1361-6595/adcb6b
[34] V.A. Lisovskiy, and V.D. Yegorenkov, Vacuum, **80**, 458 (2006). https://doi.org/10.1016/j.vacuum.2005.07.038
[35] Bh. Ramkorun, G. Chandrasekhar, V. Rangari, S. C. Thakur, R. B Comes, and E. Thomas, Plasma Sources Sci. Technol. **33,** 115004 (2024). https://doi.org/10.1088/1361-6595/ad8ae8
[36] J. Niemann, V. Schneider, and H. Kersten, Phys. Plasmas, **32**, 013510 (2025). https://doi.org/10.1063/5.0243765
[37] L. Vogelhuber, I. Korolov, M. Vass, K. Nösges, T. Bolles, K. Köhn, M. Klich, R. P. Brinkmann, and T. Mussenbrock, Plasma Sources Sci. Technol. **34**, 125012 (2025). https://doi.org/10.1088/1361-6595/ae253e
[38] D. Yang, X. Wang, Zh. Zhou, H. Li, W. Zhang, Y. Liu, J. Schulze, P. Hartmann, Z. Donkó, and Y. Fu, Appl. Phys. Letters, **127**, 124101 (2025). https://doi.org/10.1063/5.0281351
[39] B. Mahdavipour and J. T. Gudmundsson, Plasma Sources Sci. Technol. **34**, 045005 (2025). https://doi.org/10.1088/1361-6595/adc503
[40] R. Masheyeva, M. Vass, X.-K. Wang, Y.-X. Liu, A. Derzsi, P. Hartmann, J. Schulze, and Z. Donkó, Plasma Sources Sci. Technol. **33**, 045019 (2024). https://doi.org/10.1088/1361-6595/ad3c69
[41] X.-K. Wang, I. Korolov, S. Wilczek, R. Masheyeva, Y.-X. Liu, Y.-H. Song, P. Hartmann, Z. Donkó, and J. Schulze, Plasma Sources Sci. Technol. **33**, 085001 (2024). https://doi.org/10.1088/1361-6595/ad5eb9
[42] J. B. Thompson, Proc. Phys. Soc. **73**, 818 (1959). https://doi.org/10.1088/0370-1328/73/5/416
[43] A. J. Lichtenberg, V. Vahedi, M. A. Lieberman, and T. Rognlien, J. Appl. Phys. **75**, 2339 (1994). http://dx.doi.org/10.1063/1.356252
[44] E. Stoffels, W. W. Stoffels, D. Vender, M. Haverlag, G. M. W. Kroesen, F de Hoog, J. Contrib. Plasma Phys. **35**, 331 (1995). https://doi.org/10.1002/ctpp.2150350404
[45] Y. T. Lee, M. A. Lieberman, A. J. Lichtenberg, F. Bose, H. Baltes, R. Patrick, J. Vac. Sci. Technol. A, **15**, 113 (1997). https://doi.org/10.1116/1.580452
[46] S. Kim, M. A. Lieberman, A. J. Lichtenberg, and J. T. Gudmundsson, J. Vac. Sci. Technol. A **24**, 2025 (2006). http://dx.doi.org/10.1116/1.2345645
[47] V. Lisovskiy, and V. Yegorenkov, Europhysics Letters, **99**, 35002 (2012). https://doi.org/10.1209/0295-5075/99/35002
[48] C. Dominique, and C. Arnas, J. Appl. Phys. **101**, 123304 (2007). https://doi.org/10.1063/1.2748365
[49] C. Arnas, A. Mouberi, K. Hassouni, A. Michau, G. Lombardi, X. Bonnin, F. Bénédic, and B. Pégourié, J. Nuclear Materials, **390-391**, 140 (2009). https://doi.org/10.1016/j.jnucmat.2009.01.148
[50] K.K. Kumar, L. Couëdel, and C. Arnas, Phys. Plasmas, **20**, 043707 (2013). https://doi.org/10.1063/1.4802809
[51] L. Couëdel, K. Kishor Kumar, and C. Arnas, Phys. Plasmas, **21**, 123703 (2014). https://doi.org/10.1063/1.4903465
[52] S. Barbosa, F. R. A. Onofri, L. Couëdel, M. Wozniak, C. Montet, C. Pelcé, C. Arnas, L. Boufendi, E. Kovacevic, J. Berndt, and C. Grisolia, J. Plasma Phys. **82**, 615820403 (2016). https://doi.org/10.1017/S0022377816000714
[53] C. Arnas, A. Michau, G. Lombardi, L. Couëdel, and K. Kishor Kumar, Phys. Plasmas **20**, 013705 (2013). https://doi.org/10.1063/1.4776681
[54] L. Worner, E. Kovacevic, J. Berndt, H. M. Thomas, M. H. Thoma, L. Boufendi, and G. E. Morfill, New Journal of Physics, **14**, 023024 (2012). https://doi.org/10.1088/1367-2630/14/2/023024
[55] J. Beckers, J. Berndt, D. Block, M. Bonitz, P. J. Bruggeman, L. Couëdel, G. L. Delzanno, *et al*. Phys. Plasmas, **30**, 120601 (2023). https://doi.org/10.1063/5.0168088
[56] E. Kovacevic, J. Berndt, Th. Strunskus, and L. Boufendi, J. Appl. Phys. **112**, 013303 (2012). https://doi.org/10.1063/1.4731751
[57] E. Kovačević, J. Berndt, I. Stefanović, H.-W. Becker, C. Godde, Th. Strunskus, J. Winter, and L. Boufendi, J. Appl. Phys. **105**, 104910 (2009). http://dx.doi.org/10.1063/1.3129318
[58] V. A. Lisovskiy, S. V. Dudin, P. P. Platonov, S. I. Bogatyrenko, and A. A. Minenkov, Probl. At. Sci. Technol. **4**, 135 (2019), https://vant.kipt.kharkov.ua/ARTICLE/VANT_2019_4/article_2019_4_135.pdf
[59] M. Mikikian, L. Couedel, M. Cavarroc, Y. Tessier, and L. Boufendi, Eur. Phys. J. Appl. Phys. **49**, 13106 (2010). https://doi.org/10.1051/epjap/2009191
[60] M. Mikikian, S. Labidi, E. von Wahl, J. F. Lagrange, T. Lecas, V. Massereau-Guilbaud, I. Géraud-Grenier, *et al*., Plasma Phys. Control. Fusion, **59**, 014034 (2017). https://doi.org/10.1088/0741-3335/59/1/014034
[61] Sh. Amiranashvilia, and M.Y. Yu, Phys. Plasmas, **9**, 4825 (2002). https://doi.org/10.1063/1.1517049
[62] J.X. Ma, M.Y. Yu, X.P. Liang, J. Zheng, W.D. Liu, and C.X. Yu, Phys. Plasmas, **9**, 1584 (2002). https://doi.org/10.1063/1.1468234

[63] L.Z. Hadid, O. Shebanits, J.-E. Wahlund, M.W. Morooka, A.F. Nagy, and W.L. Tseng, J. Plasma Physics, **88**, 555880201 (2022). https://doi.org/10.1017/S0022377822000186
[64] V. Lisovskiy, A. Minenkov, S. Dudin, S. Bogatyrenko, P. Platonov, and V. Yegorenkov, ACS Omega, **7**, 47941 (2022). https://doi.org/10.1021/acsomega.2c05846
[65] M. Mao, J. Benedikt, A. Consoli, and A. Bogaerts, J. Phys. D: Appl. Phys. **41**, 225201 (2008). https://doi.org/10.1088/0022-3727/41/22/225201
[66] Yu.P. Raizer, *Gas Discharge Physics*, (Springer, Berlin, 1991).
[67] M. A. Lieberman, and A. J. Lichtenberg, *Principles of plasma discharges and materials processing*, (Wiley, New York, 2005).
[68] M. Keidar, and I. I. Beilis, *Plasma engineering*, (Academic Press, London, 2018).
[69] J. Berndt, E. Kovačević, I. Stefanović, O. Stepanovic, S. H. Hong, L. Boufendi, and J. Winter, Contrib. Plasma Phys. **49**, 107 (2009). http://dx.doi.org/10.1063/1.3224874
[70] D. U. B. Aussems, S. A. Khrapak, I. Dogan, M. C. M. van de Sanden, and T. W. Morgan, Phys. Plasmas, **24**, 113702 (2017). https://doi.org/10.1063/1.5001576
[71] D. Winske, and M. E. Jones, IEEE Trans. Plasma Sci. **22**, 454 (1994). https://doi.org/10.1109/27.310655
[72] S. J. Choi, and M. J. Kushner, IEEE Trans. Plasma Sci. **22**, 138 (1994). https://doi.org/10.1109/27.279017
[73] H. H. Hwang, and M. J. Kushner, J. Appl. Phys. **82**, 2106 (1997). https://doi.org/10.1063/1.366020
[74] W. Xu, N. D'Angelo, and R. L. Merlino, J. Geophys. Res. **98**, 7843 (1993). https://doi.org/10.1029/93JA00309
[75] J. Goree, and T. E. Sheridan, J. Vac. Sci. Technol. A **10**, 3540 (1992). https://doi.org/10.1116/1.577781
[76] T. E. Sheridan, J. Goree, Y. T. Chiu, R. L. Rairden, and J. A. Kiessling, J. Geophys. Res. **97**, 2935 (1992). https://doi.org/10.1029/91JA02801
[77] G. Lapenta, Phys. Plasmas, **6**, 1442 (1999). https://doi.org/10.1063/1.873395
[78] H. A. Erikson, Phys. Rev. **28**, 372 (1926). https://doi.org/10.1103/PhysRev.28.372
[79] V.A. Lisovskiy, S.V. Dudin, P. P. Platonov, and V.D. Yegorenkov, Phys. Scr. **98**, 025601 (2023). https://doi.org/10.1088/1402-4896/acae48
[80] J.C.W. Chien, *Polyacetylene: Chemistry, Physics, and Material*, (Academic Press, New York, 1984).
[81] A. M. Saxman, R. Liepins, and M. Aldissi, Prog. Polym. Sci. **11**, 57 (1985). https://doi.org/10.1016/0079-6700(85)90008-5

АМБІПОЛЯРНА ДИФУЗІЯ ТА РЕВЕРСІЯ ЗНАКУ ЕЛЕКТРИЧНОГО ПОЛЯ В ЕЛЕКТРОНЕГАТИВНІЙ ПЛАЗМІ ІЗ ЗАРЯДЖЕНИМИ НАНОЧАСТИНКАМИ

В. Лісовський, С. Дудін, С. Богатиренко, С. Резуненко, В. Єгоренков
Харківський національний університет імені В.Н. Каразіна, майдан Свободи 4, Харків, 61022, Україна

У цій роботі запропоновано аналітичну модель амбіполярної дифузії в плазмі, яка складається з електронів, позитивних і негативних іонів та негативно заряджених наночастинок. Отримані формули для коефіцієнтів амбіполярної дифузії як для кожного із сортів заряджених частинок, так і для напруженості амбіполярного електричного поля. У плазмі, що містить лише електрони та позитивні й негативні іони, за високих концентрацій негативних іонів коефіцієнти амбіполярної дифузії кожного виду заряджених частинок наближаються до коефіцієнтів їхньої вільної дифузії, тобто амбіполярна дифузія стає вільною. В плазмі з негативно заряджених наночастинок, електронів та позитивних іонів при високих концентраціях наночастинок коефіцієнт амбіполярної дифузії електронів дорівнює подвійному коефіцієнту їх вільної дифузії, а коефіцієнт амбіполярної дифузії позитивних іонів наближається до подвійного коефіцієнта вільної дифузії наночастинок. В плазмі, що складається з електронів, позитивних та негативних іонів, а також наночастинок, важливим є те, як саме втрачаються вільні електрони, тобто, будуть вони переважно утворювати негативні іони або прилипати до поверхні наночастинок. Якщо домінує прилипання електронів до молекул газу й накопичення негативних іонів, то коефіцієнти амбіполярної дифузії електронів, негативних іонів та наночастинок близькі до їхніх коефіцієнтів вільної дифузії. Якщо вільні електрони переважно зникають внаслідок їх прилипання до наночастинок, то коефіцієнти амбіполярної дифузії електронів, негативних іонів та наночастинок дорівнюють їх подвійним коефіцієнтам вільної дифузії. Виявлено, що коефіцієнт амбіполярної дифузії позитивних іонів залежить від того, як саме вільні електрони втрачаються з плазми. Якщо інтенсивно утворюються негативні іони, то він наближається до коефіцієнта вільної дифузії негативних іонів, а при інтенсивних втратах електронів на поверхні наночастинок він асимптотично зближується з подвійним значенням коефіцієнта вільної дифузії наночастинок. За наявності в плазмі достатньо високих концентрацій негативних іонів та/або заряджених наночастинок напруженість амбіполярного електричного поля суттєво зменшується й навіть може досягти нуля та змінити знак. З плазми зі слабко негативним амбіполярним полем може видалятися надлишок негативних іонів та наночастинок, які накопичуються, що стабілізує горіння розряду. Під час експериментів з ацетиленовою плазмою спостерігався потік дрібних наночастинок на стінку трубки, що може свідчити про зміну знака амбіполярного електричного поля.

Ключові слова: *амбіполярна дифузія; аналітична модель; амбіполярне електричне поле; наночастинки; негативні іони*